



Shallow Water Empirical Remote Sensing Bathymetry Using the Blue/Green and Red Spectrum Regions

Gar Al-Nabi Ibrahim Mohamed^{1*}

¹*Department of Hydrographic Surveying, Faculty of Maritime Studies, King Abdulaziz University, Kingdom of Saudi Arabia.*

Author's contribution

The sole author designed, analysed, interpreted and prepared the manuscript.

Article Information

DOI: 10.9734/JSRR/2019/v22i3330091

Editor(s):

- (1) Dr. Rahul Kumar Jaiswal, National Institute of Hydrology, WALMI Campus, Bhopal, India.
(2) Dr. Angela Gorgoglione, Department of Civil and Environmental Engineering, University of California, Davis, USA.

Reviewers:

- (1) Nguyen Ba Dai, Vietnam Academy of Sciences and Technology (VAST), Vietnam.
(2) Kefu Yu Guangxi, Guangxi University, China.
(3) Snehadri B. Ota, Institute of Physics, Sachivalaya Marg, India.

Complete Peer review History: <http://www.sdiarticle3.com/review-history/47301>

Original Research Article

Received 11 November 2018
Accepted 17 February 2019
Published 09 March 2019

ABSTRACT

An atmospherically corrected Sentinel-2 image and a 1/25000 scale nautical chart were used to investigate the performance of the electromagnetic spectrum blue/green and red regions in bathymetric data retrieval. The imaging optical empirical remote sensing bathymetry, using Stumpf (2003) reflectance model was adopted in this investigation. In clean water depth (3.1-7.3) meters both spectrum regions can be used to retrieve bathymetric data with an accuracy of $\pm (0.82-1.10)$ m. The optimum electromagnetic spectrum regions in this depth range were the blue/green spectrum range (0.457-0.523 μm) and the red range (0.773-0.793 μm). For depth range (2.1-15.5) m, the blue/green spectrum region (0.457-0.523 μm) produced better results than those of the red region. The clean water derived bathymetric data quality decreases with the increase of water depth in general and with the red spectrum region in particular. The blue/green spectrum region (0.457-0.523 μm) and the red spectrum region (0.773-0.793 μm) correlation coefficient values can be adopted as a measure of the water turbidity, using the characteristic of the water depth strong correlation in turbid water.

*Corresponding author: E-mail: gar959gar@gmail.com, gar958gar@gmail.com;

Keywords: Electromagnetic spectrum; blue/green spectrum region; red spectrum region; correlation coefficient; root mean square error; absolute mean error.

1. INTRODUCTION

1.1 Bathymetry

Water depth determination is a requirement for many processes that are applied in different fields and for different purposes, to name, but a few, navigational nautical charts, dredging operations, under water topography mapping, benthic mapping (morphology and habitat) etc. Bathymetry was traditionally dominated by the expensive, inefficient process of depth profiling using conventional depth measurement methods. Typical examples of these methods are the vessel-based graduated rods, plumb lines and echosounders. These conventional bathymetric methods are characterized by the high cost, inefficiency and inapplicability in shallow waters due to difficult navigation. However, the remote sensing methods represent a flexible, efficient and cost-effective alternative to these conventional methods. A brief informative summary of these methods was given by Gao J., who stated that "Remote sensing of bathymetry takes several forms each having its own determination depth, accuracy, strengths, limitations and best application settings". He categorized these forms into two broad categories, non-imaging and imaging methods. The latter are able to determine water depth from the radiometric properties of the captured image and the former make use of the visible light and microwave radiation [1].

This investigation was limited to the imaging optical empirical form of remote sensing bathymetry. It was carried out using shallow water multi-spectral passive satellite sensor data.

1.2 Bathymetric Models

The ability of light to penetrate the water body provides a physical basis for modelling water depth from remote sensing spectral data [2].

As the incident solar radiation propagates through the water, it is increasingly scattered and absorbed by water and in-water constituents, leaving varied energy to be scattered and recorded in remote sensing imagery. The energy received at the sensor is inversely proportional to the depth of water after atmospheric and water column effects have been removed. Therefore, the intensity of the returned signal is indicative of

the depth at which the solar radiation has penetrated [1].

Different models were used for retrieving water depth using remote sensing spectral data. Some are theoretical and based on the sophisticated transmission equation of the electromagnetic radiation in water, others are empirical and are based on the calibration between the image pixel values and their corresponding depth measured values. The semi-analytical methods integrate the empirical and theoretical methods using statistical regression.

The use of passive satellite sensor data in shallow waters is complicated by the combined atmospheric, water and bottom signals [3]. Thus, the most optimum model for retrieving water depth from remote sensing spectral data should consider, the attenuation effects resulting from the atmosphere, water body and bottom topography. However, due to the difficulties in modelling the water body and bottom topography parameters, most of the models consider the relationship between the water depth and the atmospherically corrected amount of energy leaving the water body. Typical examples of such models were those developed by Lyzenga [4] and Stumpf [5]. The last model was used in this investigation via SNAP software, Sentinel-2 toolbox. The Sentinel-2 Toolbox consists of a rich set of visualization, analysis and processing tools for the exploitation of MSI data from the upcoming Sentinel-2 mission [6]. Similar to a variety of empirical bathymetry models, Stumpf reflectance model relies on the assumption of exponential attenuation of light with depth and is based on the log transform of two bands and the derived depth z value is given by:

$$Z = m_0 * \left[\frac{\ln(n * R_i)}{\ln(n * R_j)} \right] - m_1$$

where,

n is a constant to ensure positive value after the log transform and a linear relationship between the ratio and the depth.

R_i and R_j are atmospherically corrected reflectance values in the two bands i and j .

m_1 is a tunable constant to scale the ratio to depth and m_0 is an offset value when z equals zero.

1.3 Optimal Bathymetric Bands

The selection of optimal electromagnetic spectrum for bathymetric modelling is important for obtaining reliable bathymetric results from the spectral remote sensing data.

Never-the less, the short wavelength algorithms advocated for bathymetric measurements in clear water can not be applied to turbid productive water. Turbid waters shift the optimum wavelength of sensing bathymetry towards longer radiation away from the vicinity of 0.45 μm that tends to have the maximum penetration in clear water [7]. In this environment water depth is strongly correlated with the red band of 0.746-0.759 μm range, but not the blue end of the spectrum [8,1].

Due to the lack of information related to water turbidity in the study area, both the blue and red ends of the electromagnetic spectrum will be used to retrieve bathymetric data to elaborate on the performances of the different portions of the spectrum in this specific spectrum range.

2. METHODOLOGY

2.1 The Study Area

The study area lies in the Gulf of Aden, Yemen, Aden Harbor and approaches. It is covered by the nautical chart sheet 7, published at Taunton U.K., July 1884, under the superintendence of Rear Admiral Sir David K.E.C.B., Hydrographer of the Navy, Edition 26th August, 1999, [9]. Two test areas covered by this nautical chart were used in this investigation and the water depths ranged between 3.1 and 7.3 meters in the first area (area1) and between 2.1 to 15.5 meters in the second area (area2) (Fig. 1). The bathymetric layer of the study area was derived using Sentinel-2 image and the depth values of the calibration points were retrieved using the derived bathymetric layer. The performance of the specific electromagnetic spectrum portion in the blue/green and red regions was obtained by the quality assessment method highlighted in section 3.2.

2.2 Data Sets

The data sets used in this investigation included an atmospherically corrected 10 m resolution Sentinel-2 satellite image, and a 1/25000 scale nautical chart (Fig. 1).

Sentinel-2 is a wide-swath, high resolution multi-spectral imaging mission supporting, Copernicus land monitoring studies, including the monitoring of vegetation, soil and water cover as well as observation of inland waterways and coastal areas. The Sentinel-2 multi-spectral instrument (MSI) samples 13 spectral bands, four bands at 10 meters, six bands at 20 meters and three bands at 60 meters spatial resolution, Table 1, [10].

3. WATER DEPTH RETRIEVAL AND FORMATION OF BATHYMETRIC BAND

3.1 Formation of Bathymetric Bands

The blue/green spectrum region provides the higher water penetration for improved bathymetry retrieval [3]. Spectral bands of short wavelengths are preferred in bathymetric mapping from space as there is low attenuation from electromagnetic radiation [1]. As quoted in section 3, both the blue/green and red regions of the electromagnetic spectrum can be used for water depth retrieval and the decision as to which region to use depends on the water turbidity. The main problem here is the lack of information related to water turbidity in the large water areas covered by the satellite multi-spectral imagery. This paper considered the use of both regions to derive a shallow water bathymetric layer, adopting the reflectance ratio model developed by Stumpf et al. [5]. This would facilitate an insight elaboration in the performance of the different portions of the electromagnetic spectrum in these regions. The spectrum portions used are based on Sentinel-2 bands wavelengths and spatial resolutions (Table 1). A total of nine reflectance ratio models was formed, one blue/green model, four blue/red models and four green/red models. The bathymetric layer of test area 1, was derived using these nine models, the Sentinel-2 atmospherically corrected image and a total of 16 calibration points extracted from the 1/25,000 scale nautical chart of the area. A typical example of the blue/red models derived bathymetric bands, is presented in Fig. 2.

3.2 Quality Assessment of Derived Bathymetric Data

The quality assessment of the derived bathymetric data was based on the calibration points extracted from the 1/25,000 nautical chart of the study area. It was carried out by comparing the calibration points derived and nautical chart extracted corresponding data

values, using simple statistical models. The statistical models adopted in this investigation are, the root mean square error (RMSE), correlation coefficient (r), mean absolute error (MAE) and maximum error (ME) (equations 1, 2 and 3) below:

$$RMSE = \sum_{i=0}^n (x_i - y_i)^2 / n \quad (1)$$

$$MAE = \sum_{i=1}^n abs(x_i - y_i) / n \quad (2)$$

$$r = \frac{\sum_{i=1}^n (x_i - x_0) * (y_i - y_0)}{\sqrt{\sum_{i=1}^n (x_i - x_0)^2 * \sum_{i=1}^n (y_i - y_0)^2}} \quad (3)$$

x_i is the calibration point derived depth value,
 y_i is the calibration point nautical chart depth value,

x_0 is the mean of the derived depth values.

y_0 is the mean of the nautical chart values.



Fig. 1, Part of the nautical chart showing, the study area, and the two test areas, bounded red.

Table 1. Sentinel-2 bands wavelength and spatial resolution

Band name	Resolution (m)	Central wavelength (nm)	Band width (nm)	Band range (nm)	Purpose
B01	60	443	20	433-453	Aerosol
B02	10	490	65	457.5-522.5	Blue
B03	10	560	35	577.5-667.5	Green
B04	10	665	30	650-680	Red
B05	20	705	15	697.5-712.5	Vegetation classification
B06	20	740	15	732.5-747.5	Vegetation classification
B07	20	783	20	773-793	Vegetation classification
B08	10	842	115	784.5-899.5	Near infrared
B08A	20	865	20	855-875	Vegetation classification
B09	60	945	20	935-955	Water vapor
B10	60	1375	30	1360-1390	Cirrus
B11	20	1610	90	1615-1655	Snow/ice/cloud discrimination
B12	20	2190	180	2100-2280	Snow/ice/cloud discrimination

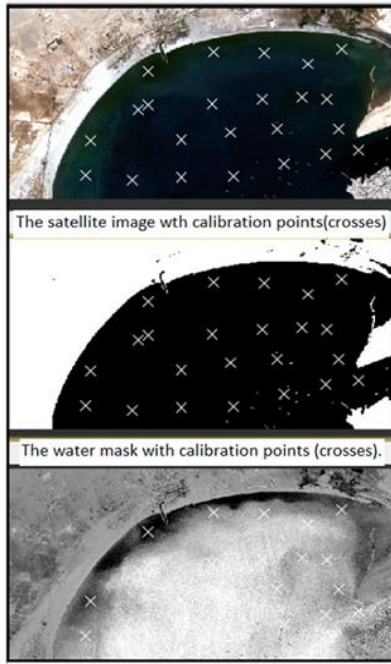


Figure 2, A typical example of an imagery derived bathymetric band of the blue/red spectrum region models, the satellite image (upper) and the water mask (middle).

4. RESULTS

4.1 Test Area1 Results

The results obtained for test area 1, are presented in Table 2, which shows, the Model Number (MN), reflectance ratio bands, Root Mean Square Error (RMSE), correlation coefficient (r) and maximum error value (ME).

The statistical results for test area1, Table 2, showed that the RMSE values vary from 0.82 to 1.1 meters, with the maximum value associated with the blue/green model 1, while the AME values vary from 0.77 to 0.97 meters, with the minimum value associated with the same model. The high correlation value was delivered by the blue/green region, model1 (0.68) and may suggest that the water was not turbid [7]. Although all the red region models delivered similar performances with respect to the RMSE and MAE statistical parameters, but the correlation coefficient and maximum error values demonstrated bad performances for the blue/green model 2 and the green/red model 6. The red spectrum region green/red models 5,6 and 7, delivered the best performances with respect to all the statistical measures. This clearly revealed that the best performance of the two

tested spectrum regions was recorded by the red electromagnetic spectrum portion (0.6975-0.793 μm). This almost agreed with the red band wavelength width given by George, (0.746-0.759 μm), [8]. Though the red region models performed better than the blue/green region model, these results demonstrated that both the regions can be used for depth retrieval in the applied depth range (3.1-7.3 meters), as the difference between the red region models average RMSE value and the blue/green region value is only 24 cm (1.1-.86 m). The green/blue model1 performed better than all the red region models with respect to the correlation coefficient and absolute mean error values (0.68, 0.77 m). Also, this model delivered a low maximum error value compared to the red region models (2.38 m), with an exception of the green/red model 7, which delivered a value better than the blue/green model1 (1.92 m).

The results for test area1 demonstrated the performances of the blue/green and red spectrum regions in a depth range of 3.1 to 7.3 meters. In order to elaborate more in the performances of these two spectrum regions the same nine models were applied in test area2 with a depth range of 2.1 to 15.5 meters.

4.2 Test Area2 Results

The results obtained for test area2 are presented in Table 3.

The statistical results in Table 3, showed RMSE, correlation coefficient, and mean absolute error values ranging from 1.74 to 1.93 m, 0.5 to 0.79 and 1.27 to 1.47 m respectively. These results indicated that the best performance was delivered by the blue/green region model1, which records the best values for all statistical measures in general and the maximum error value in particular (3.51 m). This value in fact credited the blue/green model, compared to all the red region models' values, which ranged between 3.90 and 5.79 meters. The blue/green region maximum correlation value (0.79) suggested that the water was not turbid at the moment of Sentinel-2 image recording, otherwise the water depth would be strongly correlated with the red region models [7]. The red region models delivered good performances with respect to the statistical parameters, but recorded large maximum error values that ranged between 3.90 to 5.79 meters. Compared to area 1, maximum error values (1.92-2.38) recorded in Table 3, these values demonstrated the increase of the maximum error values with the depth increase.

Table 2. The results obtained for test area1, applying the nine models

MN	Ratio bands	RMSE (m)	AME(m)	r	ME (m)	Remarks
1	B2-B3	1.10	0.77	0.68	2.38	Blue/Green
2	B2-B4	0.93	0.97	0.19	2.83	Blue/Red
3	B2-B5	0.80	0.92	0.20	2.56	Blue/Red
4	B2-B6	0.85	0.88	0.23	2.74	Blue/Red
5	B2-B7	0.82	0.85	0.27	2.64	Blue/Red
6	B3-B4	0.83	0.88	-0.07	2.76	Green/Red
7	B3-B5	0.86	0.79	0.56	1.92	Green/Red
8	B3-B6	0.90	0.79	0.50	2.38	Green/Red
9	B3-B7	0.86	0.78	0.50	2.36	Green/Red

Table 3. The results obtained for test area 2, applying the nine models

MN	Ratio bands	RMSE (m)	AME (m)	r	Maximum error	Remarks
1	B2-B3	1.74	1.43	0.79	3.51	Blue/Green
2	B2-B4	1.77	1.42	0.53	5.06	Blue/Red
3	B2-B5	1.90	1.42	0.59	4.45	BLUE/Red
4	B2-B6	1.78	1.47	0.50	5.79	Blue/Red
5	B2-B7	1.86	1.45	0.52	4.87	Blue/Red
6	B3-B4	1.83	1.33	0.66	3.90	Green/Red
7	B3-B5	1.93	1.27	0.68	4.11	Green/Red
8	B3-B6	1.80	1.42	0.59	5.18	Green/Red
9	B3-B7	1.88	1.36	0.60	4.24	Green/Red

5. VISIBLE LIGHT WATER PENETRATION

Light water penetration decreases with the decrease of the light energy. The amount of light energy depends on the band wavelength and the shorter the wave the higher the energy. Different visible light wavelengths penetrate to different depths depending on water condition, wave energy and absorptivity. Most of the visible light spectrum is absorbed within 10 meters (33 feet) of the water's surface, and almost none penetrates below 150 meters (490 feet) of water depth, even when the water is very clear [11]. This demonstrated that all the visible light bands are approximately equally absorbed up to the depth of 10 meters.

The long wavelengths of the light spectrum—red, yellow, and orange—can penetrate to approximately 15, 30, and 50 meters (49, 98, and 164 feet), respectively, while the short wavelengths of the light spectrum—violet, blue and green—can penetrate further, to the lower limits of the euphotic zone [11]. This is clearly demonstrated in Fig. 3 [12] which revealed the water depth penetrations for the visible light spectrum in clean ocean water and turbid coastal water. The penetration depths of the blue, green and red bands waves in turbid coastal water are approximately, 30, 55 and 25 meters respectively, but can reach up to 205, 105 and

50 meters respectively in clean ocean water. The depths tested in the investigation ranged between 2.1 and 15.5 meters and the tested regions (blue/green and red) can penetrate these depths with almost equal absorption attenuation up to 10 meters [11]. Therefore, the tested regions have no energy and absorptivity constraints up to the maximum tested depth (15.5). The water turbidity effect depends on the presence of solid particles in the water column and the tested spectrum regions are affected differently, due to light scattering and absorption characteristics. The turbidity attenuation would increase with the depth but the amount of energy would decrease. The energy received at the sensor can be modelled to retrieve the water depth if the atmospheric, water column and bottom topography effects are removed. The multi-spectral data used in this investigation was atmospherically corrected, the bottom topography noise was reduced applying filtering operations and the water column effect was considered by the adopted bathymetric model parameters m_0 and m_1 .

6. DISCUSSION

The results obtained for the two test areas, (area1 and area2) demonstrated strong depth correlation with the blue/green region (0.68, 0.79). For test area1 (Table 3), weak depth

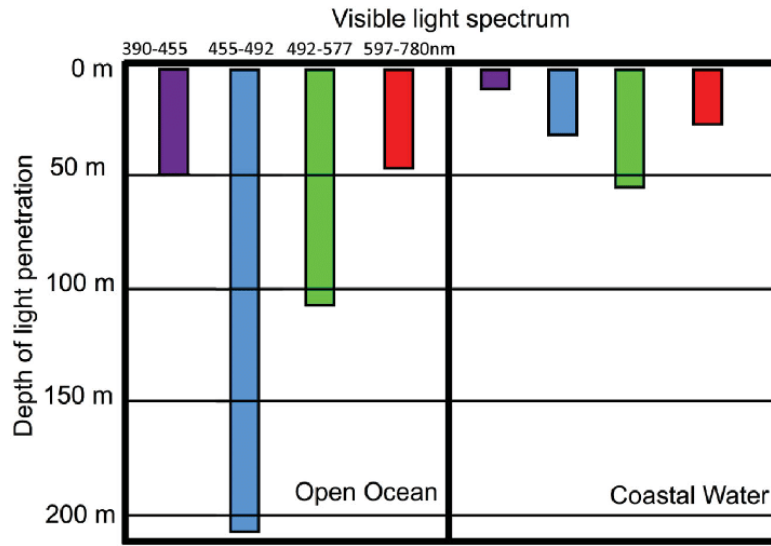


Fig. 3. The penetration depth of the visible light spectrum in clear oceanic waters compared with turbid coastal waters. Adapted with permission. 103 [13], Copyright 2016, NOAA Ocean Explorer [12]

correlation (0.19-0.27) and large maximum error values (2.64-2.83) were associated with the red spectrum region models blue/red models 2, 3, 4 and 5 and green/red model 6. The green/red models 7, 8 and 9 delivered good correlation coefficient values (0.5-0.56) and maximum error values (1.92-2.38). The green/red model 6 was the only model recorded a negative correlation coefficient value (-0.07) but associated with good absolute mean error value (0.88). Though the best performance for test area1 was recorded by the blue/green model1, but the green/red models 7, 8 and 9 delivered an acceptable performance. This revealed that both the blue/green spectrum region (0.457-0.523 μ) and red spectrum region (0.698-0.793 μ) can be used to retrieve bathymetric data for clean water depth range of 3.1-7.3 meters.

For test area2, the best performance with respect to all the statistical parameters was obtained by the blue/green region model1 (1.74, 1.43, 0.79 and 3.51). The red region model's performance was good with an exception of the maximum error values (3.90-5.79). These results clearly demonstrated that, for depth range (2.1-15.5) meters, the blue/green spectrum region is better than the red region with respect to all the statistical parameters in general and the maximum error value in particular. Thus, for clean water depth range (3.1-7.3) m both regions can be used to retrieve bathymetric data, but for depth range (2.1-15.5) meters, the blue/green

spectrum region is preferred. The strong correlation of depth with the blue/green spectrum region suggested that the water turbidity was not enough to shift the depth correlation from the blue/green region to the red region. The blue/green spectrum region (0.457-0.523 μ) and the red spectrum region (0.773-0.793 μ) correlation coefficient values can be adopted as a measure of the water turbidity.

7. CONCLUSIONS

In clean water depth range (3.1- 7.3) meters, both the blue/green region (0.457-0.523 μ) and the red region (0.773-0.793 μ) can be used for bathymetric data retrieval, using the empirical form of remote sensing bathymetry. The best log ratio division band for both regions is band 3 (0.578-0.668 μ). For water depth (2.1-15.5) meters, the blue/green spectrum region (0.457-0.523 μ) was the optimum. The conclusions derived from this investigation are, the nine models adopted, with different band combinations can be used to retrieve bathymetric data for depth range 3.1 to 7.3 meters, the blue/green spectrum region is optimum for depth range 2.1 to 15.5 meters. Also, the blue/green spectrum region (0.457-0.523 μ) and the red spectrum region (0.773-0.793 μ) correlation coefficient values can be adopted as a measure of the water turbidity, using the characteristic of the water depth strong correlation in turbid water.

ACKNOWLEDGEMENT

This research is fully supported by the deanship of scientific research, King Abdulaziz University.

COMPETING INTERESTS

Author has declared that no competing interests exist.

REFERENCES

1. Gao J. Bathymetric mapping by means of remote sensing: Methods, accuracy and limitations. *Progress in Physical Geography*. 2009;33(1):103-116.
2. Zhongwei Deng, Minhe Ji, Zhihua Zhang. Mapping bathymetry from multi-source remote sensing images: A case study in the Beilun Estuary, Guangxi, China. *The International Archives of the Photogrammetry, Remote Sensing and Spatial Information Sciences*. Beijing. 2008;37(Part B8).
3. William J. Hernandez, Roy A. Armstrong. Deriving bathymetry from multispectral remote sensing data. *Journal of Marine Science and Engineering*; 2016. DOI: 10.3390/jmse4010008
4. Lyzenga DR. Passive remote sensing techniques for mapping water depth and bottom features. *Appl Opt*. 1978;17(3):379-383. DOI: 10.1364/AO.17.000379
5. Stumpf RP, Holderied K, Sinclair M. Determination of water depth with high-resolution satellite imagery over variable bottom types. *Limnology and Oceanography*. 2003;48(1):547-556.
6. Available: <https://sentinel.esa.int/web/sentinel/toolboxes/sentinel-2>
7. Siegal BS, Gillespie AR. *Remote sensing in geology*. New York: Wiley; 1980.
8. George DG. Bathymetric mapping using a compact airborne spectrographic imager (CASI). *International Journal of Remote Sensing*. 1997;18:2067-71.
9. Nautical chart No. 7, Yemen, Aden Harbor and approaches. The Kingdom Hydrographic Office, Taunton, Somerset TA1 2DN, U.K.
10. Available: <https://sentinel.esa.int/web/sentinel/missions/sentinel-2>
11. Available: <http://www.waterencyclopedia.com/La-Mi/Light-Transmission-in-the-Ocean.html>
12. Available: <https://www.researchgate.net/figure/The-penetration-depth-of-the-visible-light-spectrum-in-clear-oceanic-waters-compared>
13. Available: <https://www.law.cornell.edu/uscode/text/17/103>

© 2019 Mohamed; This is an Open Access article distributed under the terms of the Creative Commons Attribution License (<http://creativecommons.org/licenses/by/4.0>), which permits unrestricted use, distribution, and reproduction in any medium, provided the original work is properly cited.

Peer-review history:

The peer review history for this paper can be accessed here:
<http://www.sdiarticle3.com/review-history/47301>